

A minimal model for flow control with a poro-elastic coating

Divya Venkataraman, Alessandro Bottaro & Rama Govindarajan*

* On leave from JNCAS, Bangalore

**ERCOFTAC Symposium on UNSTEADY SEPARATION IN
FLUID-STRUCTURE INTERACTION
Mykonos, Greece, 17-21 June 2013**

WHY “POROELASTIC”?

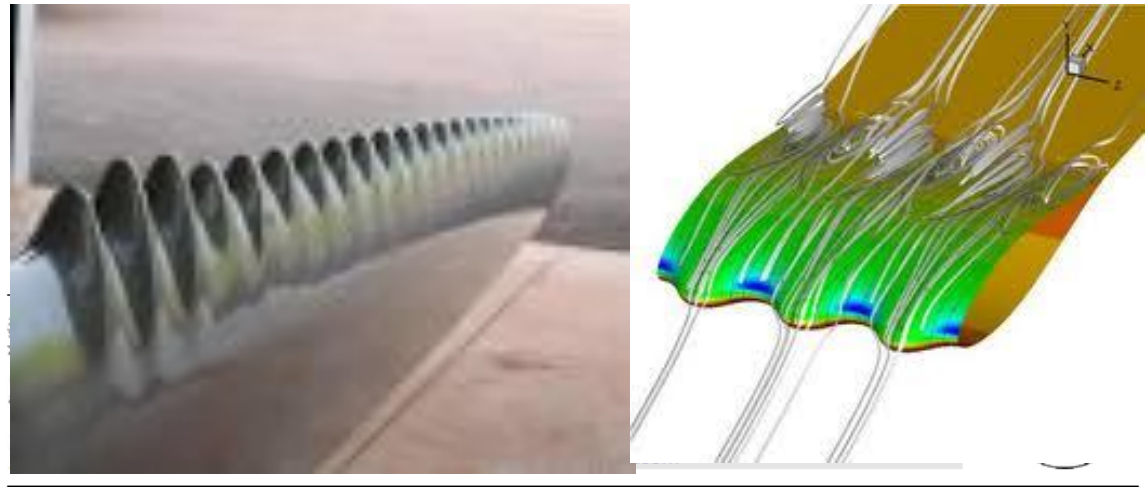
**BECAUSE IN NATURE ROUGH, COMPLIANT, FUZZY, ETC.
IS THE RULE, WHEREAS RIGID AND SMOOTH IS NOT!**

Passive flow control

Problem motivation

Examples in nature abound

leading edge undulations, i.e. tubercles on whales' flippers



Biomimetic flow control

Control of the separated flow around an airfoil using a wavy leading edge inspired by humpback whale flippers

Contrôle du décollement autour d'un profil d'aile présentant un bord d'attaque ondulé inspiré des ailerons de la baleine à bosse

Julien Favier^{a,*}, Alfredo Pinelli^a, Ugo Piomelli^b

^a CIEMAT, Unidad de Modelización y Simulación Numérica, 28040 Madrid, Spain

^b Dept. of Mechanical and Materials Engineering, Queen's University, Kingston (Ontario) K7L 3N6, Canada

Passive flow control

Problem motivation

Examples in nature abound

leading edge undulations, i.e. tubercles on whale's flippers

multi-winglets, spiroid winglets, i.e. primary remiges



ELSEVIER

Nick Dunlap

www.sciencedirect.com

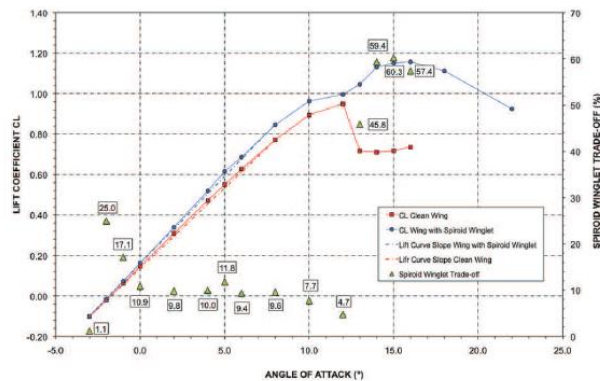


Fig. 10. Lift coefficient versus angle of attack for the clean wing (CW) and the wing with the spiroid wingtip (WSW).

Biomimetic flow control

Biomimetic spiroid winglets for lift and drag control

Joel E. Guerrero*, Dario Maestro, Alessandro Bottaro

University of Genoa, Department of Civil, Environmental and Architectural Engineering, DICAT, Via Montalegno 1, 16145 Genoa, Italy

ARTICLE INFO

Article history:
Available online 30 December 2011

Keywords:
Computational fluid mechanics
Spiroid winglets

ABSTRACT

In aeronautical engineering, drag reduction constitutes a challenge and there is room for improvement and innovative developments. The drag breakdown of a typical transport aircraft shows that the lift-induced drag can amount to as much as 40% of the total drag at cruise conditions and 80–90% of the total drag in take-off configuration. One way of reducing lift-induced drag is by using wingtip devices. By applying biomimetic abstraction

Passive flow control

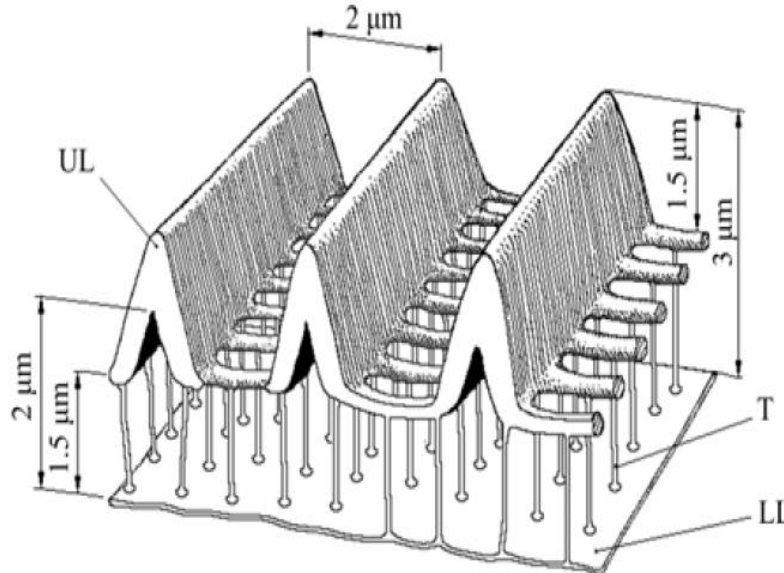
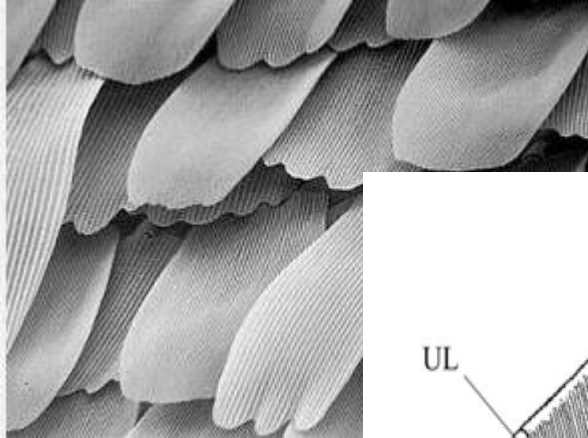
Problem motivation

Examples in nature abound

leading edge undulations, i.e. tubercles on whale's flippers

multi-winglets, i.e. primary remiges

porous riblets on butterfly and moth scales (on the wings)



WIND ENGINEERING VOLUME 34, No. 4, 2010 PP 351-360

“From Butterfly to Wind Turbine”

Igor Kovalev

Kinneret College on the Sea of Galilee, Emek Hayarden 15132, Israel

kovis@ashdot-m.org.il

ABSTRACT

The lift force and vibration performance of a wind turbine blade with a porous riblet structure (metallic version of the butterfly scale) were experimentally investigated. The study was initially directed to this problem by observation of the complex morphology of butterfly scales.

Passive flow control

Problem motivation

Examples in nature abound

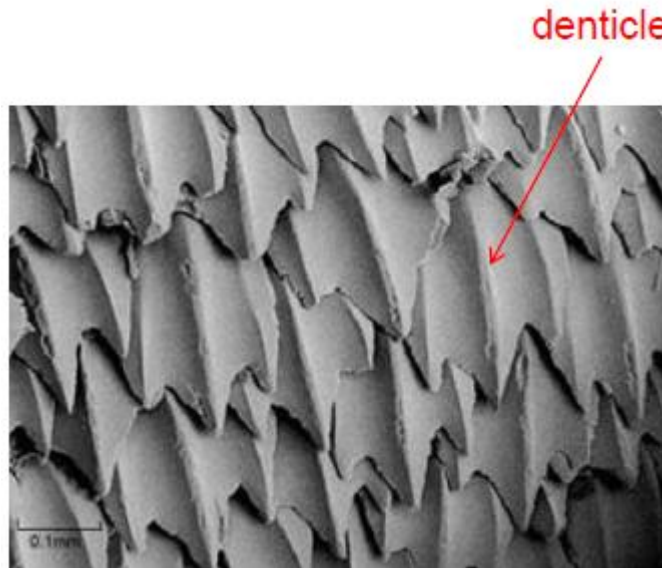
leading edge undulations, i.e. tubercles on whale's flippers

multi-winglets, i.e. primary remiges

porous riblets on butterfly and moth scales (on the wings)

denticles on shark skin

785



The Journal of Experimental Biology 215, 785-795
© 2012. Published by The Company of Biologists Ltd
doi:10.1242/jeb.063040

RESEARCH ARTICLE

The hydrodynamic function of shark skin and two biomimetic applications

Johannes Oeffner and George V. Lauder*

Museum of Comparative Zoology, Harvard University, 26 Oxford Street, Cambridge, MA 02138, USA

*Author for correspondence (glauder@oeb.harvard.edu)

Accepted 16 November 2011

SUMMARY

It has long been suspected that the denticles on shark skin reduce hydrodynamic drag during locomotion, and a number of man-made materials have been produced that purport to use shark-skin-like surface roughness to reduce drag during swimming. But no studies to date have tested these claims of drag reduction under dynamic and controlled conditions in which the swimming speed and hydrodynamics of shark skin and skin-like materials can be quantitatively compared with those of controls lacking surface ornamentation or with surfaces in different orientations. We use a flapping foil robotic device that allows accurate determination of the self-propelled swimming (SPS) speed of both rigid and flexible membrane-like foils made of shark skin and two biomimetic models of shark skin to measure locomotor performance. We studied the SPS speed of real shark skin, a silicone riblet material with evenly spaced ridges and a Speedo® 'shark skin-like' swimsuit fabric attached to rigid flat-plate foils and when made into flexible membrane-like foils. We found no consistent increase in swimming speed with Speedo® fabric, a 7.2% increase with riblet material, whereas shark skin membranes (but not rigid shark skin plates) showed a mean 12.3% increase in swimming speed compared with the same skin foils after removing the denticles. Deformation of the shark skin membrane is thus crucial to the drag-reducing effect of surface denticles. Digital particle image velocimetry (DPIV) of the flow field surrounding moving shark skin foils shows that skin denticles promote enhanced leading-edge suction, which might have contributed to the observed increase in swimming speed. Shark skin denticles might thus enhance thrust, as well as reduce drag.

Key words: shark skin, locomotion, riblet, drag reduction, foil, swimming, Fastskin®.

Passive flow control

Problem motivation

Examples in nature abound

leading edge undulations, i.e. tubercles on whale's flippers

multi-winglets, i.e. primary remiges

porous riblets on butterfly and moth scales (on the wings)

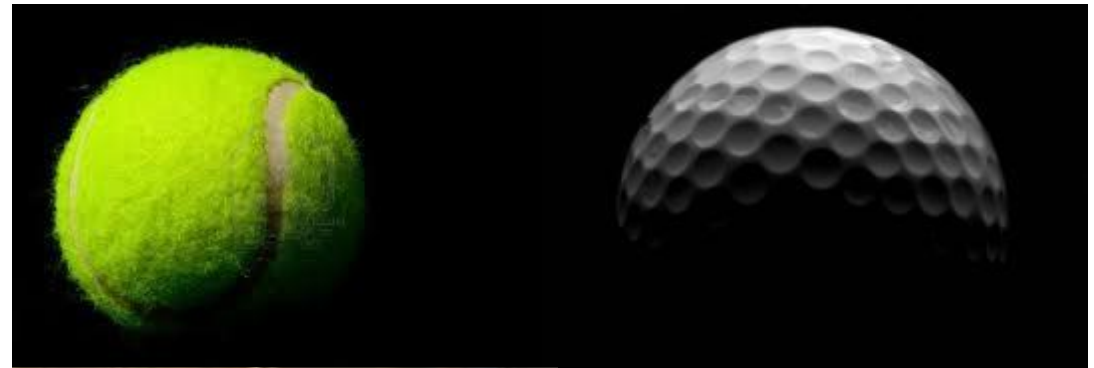
denticles on shark skin

as well as in sports

fuzz on a tennis ball

dimples on a golf ball

...



Passive flow control

Problem motivation

- ***Focus*** of this work: *covert feathers* (layer of self-actuated flaps).
- ***Passive*** “pop-up” of coverts on wings of some birds during
 - landing and gliding phases of flight, perching manoeuvres;
 - in general - high angle-of-attack/ low-lift regimes.



the Mykonos pelican

Passive flow control with a poro-elastic coating

A rapid research survey

AIM: *Determine structure parameters of feathers that yield “optimal” fluid-dynamical performance.*

Experiments

Poroelasticity
theory

NS IBM
simulations

Low order
model

- Berlin, Rechenberg,
- Freiberg, Brücker,
- Orléans, Kourta,
- Genova,
- Oxford, Taylor,
- Palaiseau, de Langre, ...

- Genova (at low Re number) :
Favier et al., 2009
Venkataraman & Bottaro, 2012
- Favier (AMU), Revell
(Manchester), Pinelli (City U.)

Gopinath & Mahadevan, 2010

Present work
+
Ongoing research...

Outline

- ***Computational modeling of fluid-structure interaction***
 - Highlights of numerical procedure
 - Key computational results
- ***Theoretical modeling for vortex-shedding***
 - ***Smooth airfoil***
 - Development of the minimal model
 - Calibration against CFD results
 - ***Airfoil with poro-elastic coating (“hairfoil”)***
 - Motivation & development
 - Results, comparison with CFD & *physical* indications
- ***Summary & future extensions***

Computational modeling of fluid-structure interaction

Highlights of numerical procedure

Key computational results

Theoretical modeling for vortex-shedding

Smooth airfoil

Development of the minimal model

Calibration against CFD results

- ***Airfoil with poro-elastic coating (“hairfoil”)***

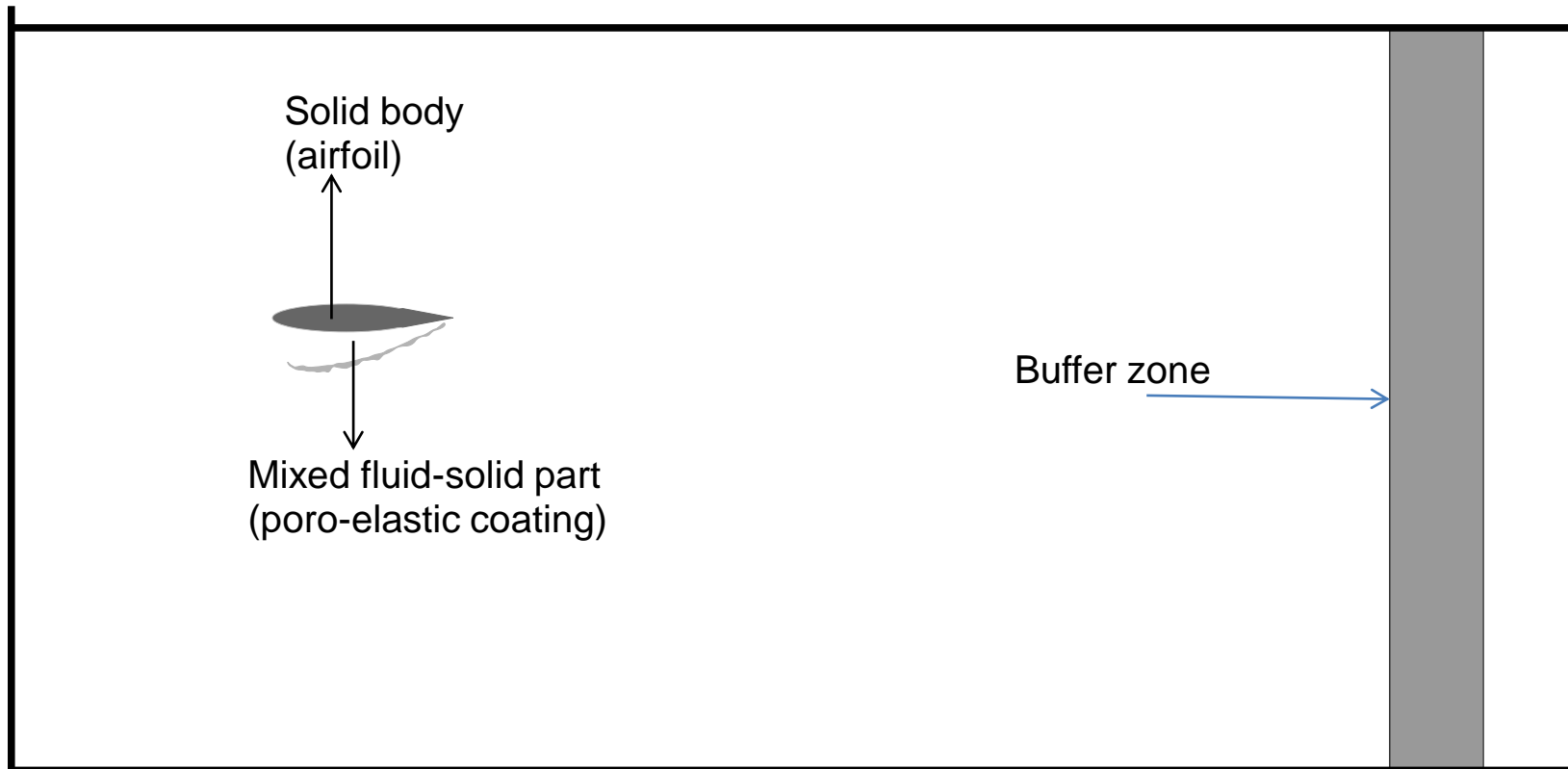
Motivation & development

Results, comparison with CFD & *physical* indications

Computational model

Fluid solver (developed by Antoine Dauptain & Julien Favier)

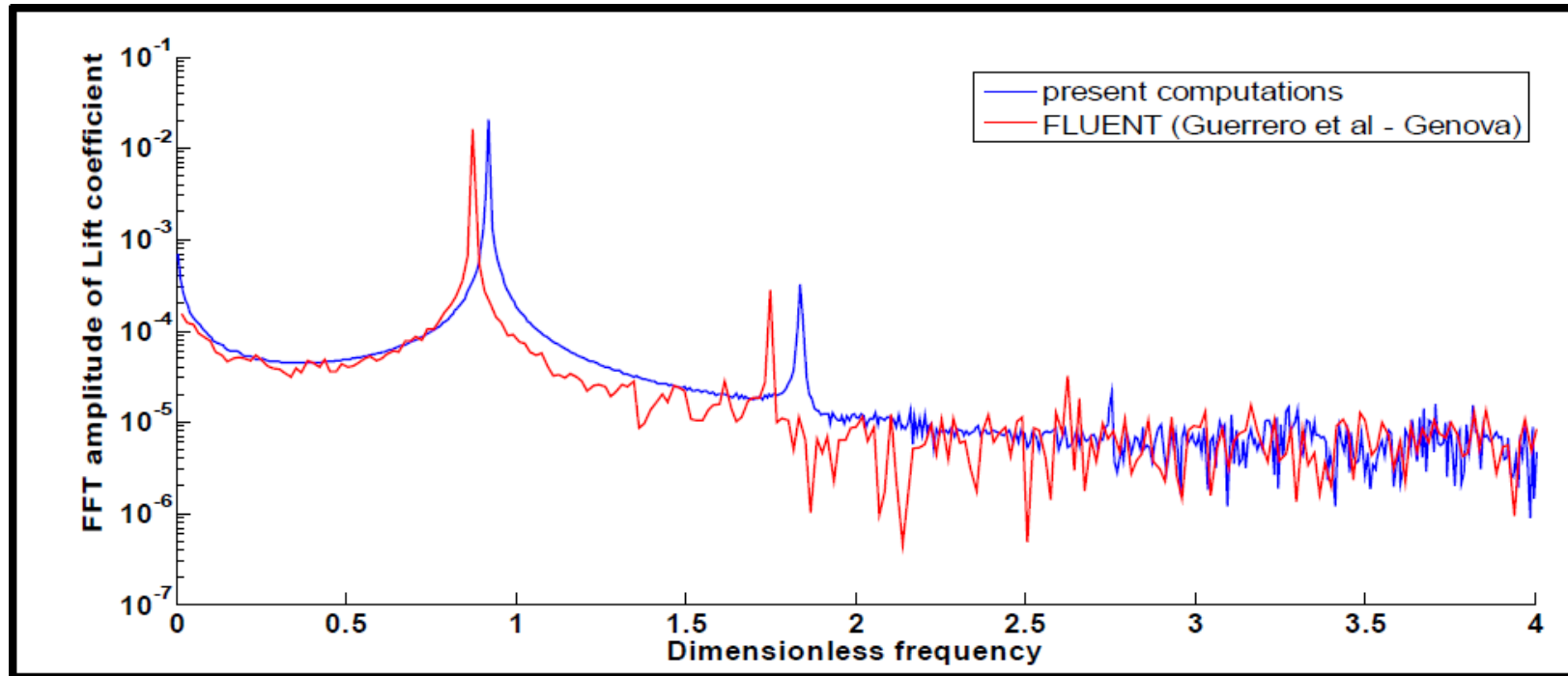
- **2-D** computations – **NACA0012 airfoil**.
- $Re = 1100$ for this study – **low Reynolds** number regime.
- **Immersed boundary forces** – for airfoil, buffer zone, coating.
- Hence, **fixed Cartesian grid** (fine on and near airfoil).
- **Numerical scheme** :
 - Convective part - explicit Adams-Bashforth
 - Viscous part - semi-implicit Crank-Nicolson
 - Pressure Poisson - conjugate gradient



Validation of fluid solver

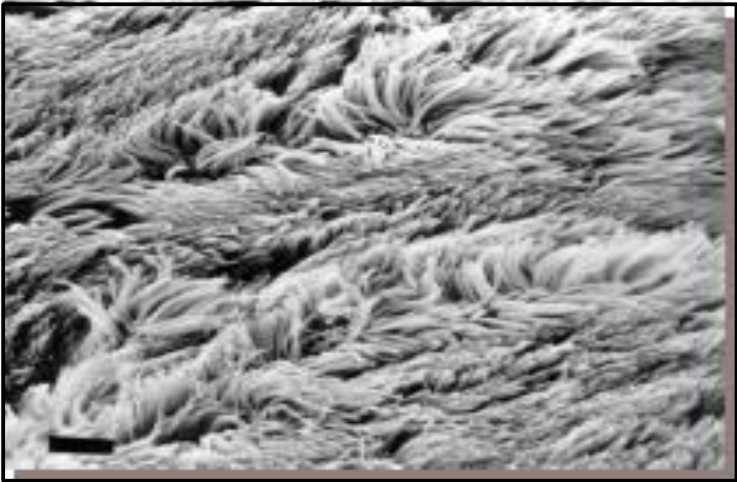
Case : 10° angle of attack

COMPARISON OF FREQUENCY SPECTRA



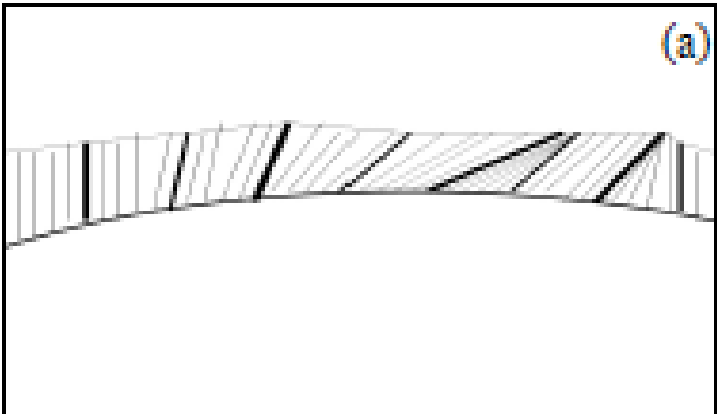
- **Qualitative analysis:**
 - Periodic solutions **sinusoidal**
 - similar frequency spectra – **peak at 2nd superharmonic** of fundamental frequency.
- **Quantitative analysis:** Close values of
 - **mean lift**
 - **frequency** of oscillations.

• **Fluid** → **structure forcing & vice-versa**

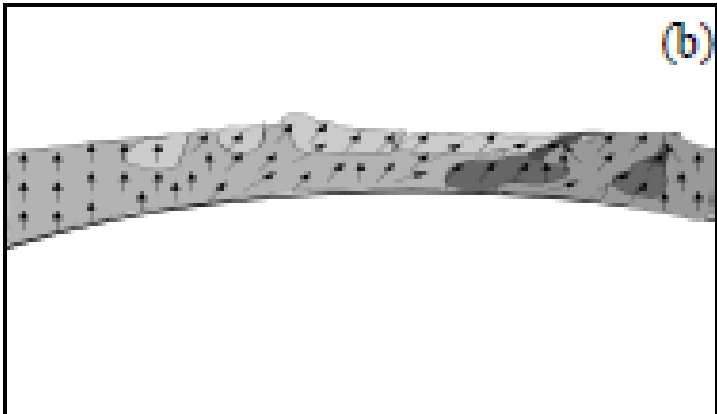


• Modeling all the feathers – too heavy.... Hence,

Homogenized approach

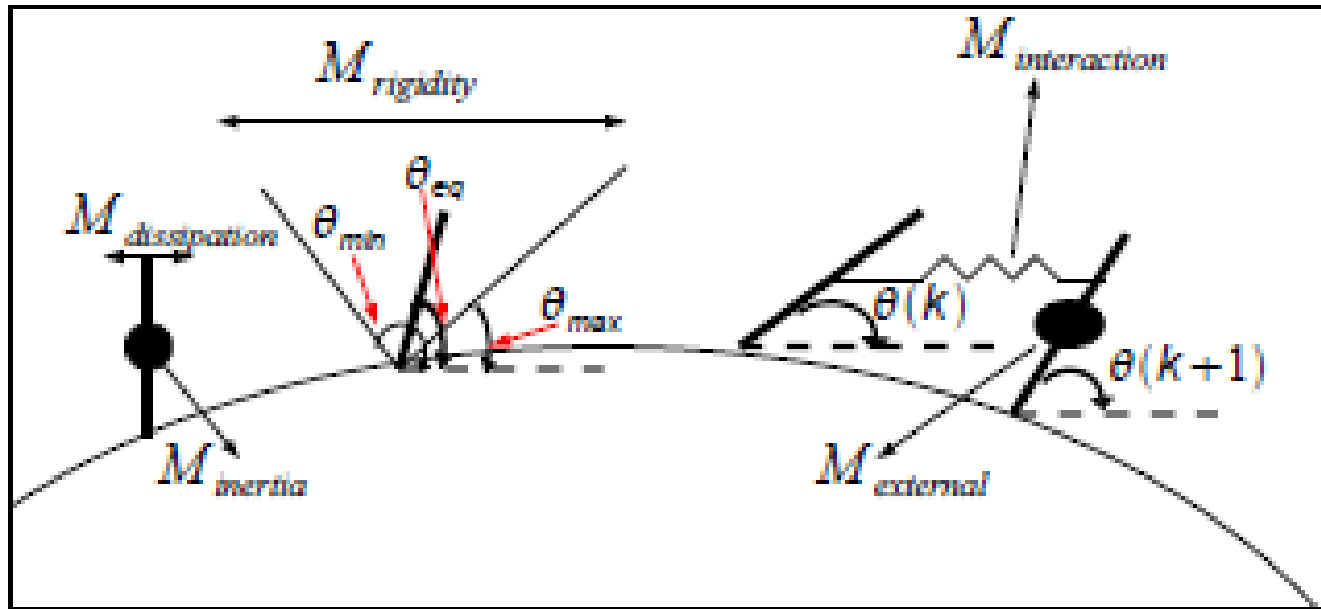


Varying porosity & anisotropy



- Normal component of the force: **Koch & Ladd** (*JFM*, 1997)
- Tangential component: **Stokes' flow** approx (Favier et al. *JFM*, 2009)

Structure solver



- For **each reference feather**, equation for **momentum balance** solved.

$$M l_c^2 \ddot{\theta} + K_r f_1(\theta) + K_i f_2(\theta) + K_d \dot{\theta} = l_c F_{ext}$$

- **Different frequency scales** (\equiv time scales) :

$$\omega_r = \sqrt{\frac{K_r}{M l_c^2}}; \omega_i = \sqrt{\frac{K_i}{M l_c^2}}; \omega_d = \frac{K_d}{M l_c^2}$$

- In present problem, **rigidity effects dominant** - i.e.,

$$\omega_d < \omega_i < \omega_r$$

Computational modeling of fluid-structure interaction

Highlights of numerical procedure

Key computational results

Theoretical modeling for vortex-shedding

Smooth airfoil

Development of the minimal model

Calibration against CFD results

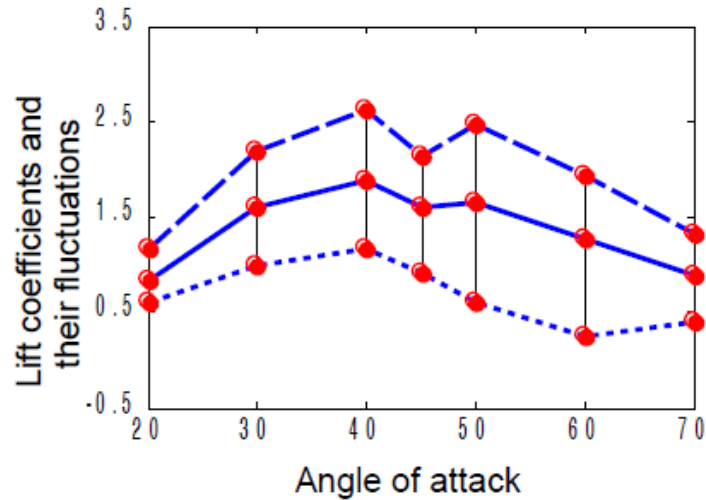
- ***Airfoil with poro-elastic coating (“hairfoil”)***

Motivation & development

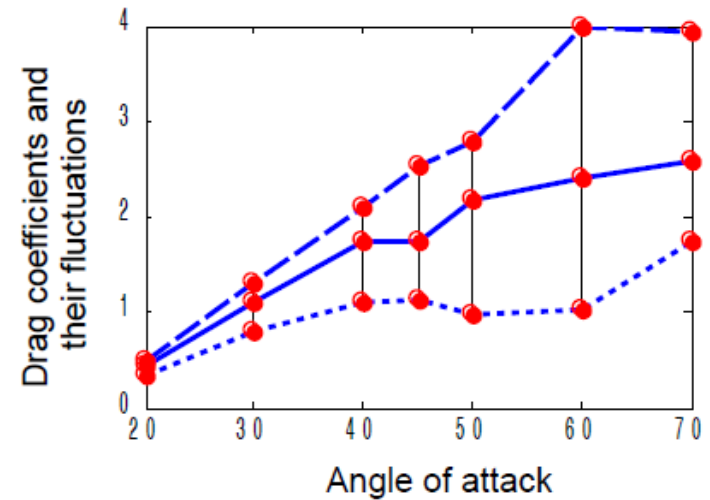
Results, comparison with CFD & *physical* indications

RESULTS : Smooth airfoil case

Mean lift vs. angle of attack

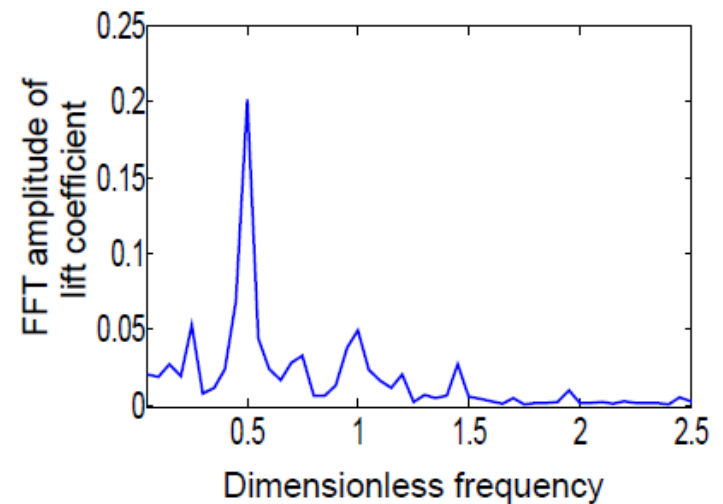
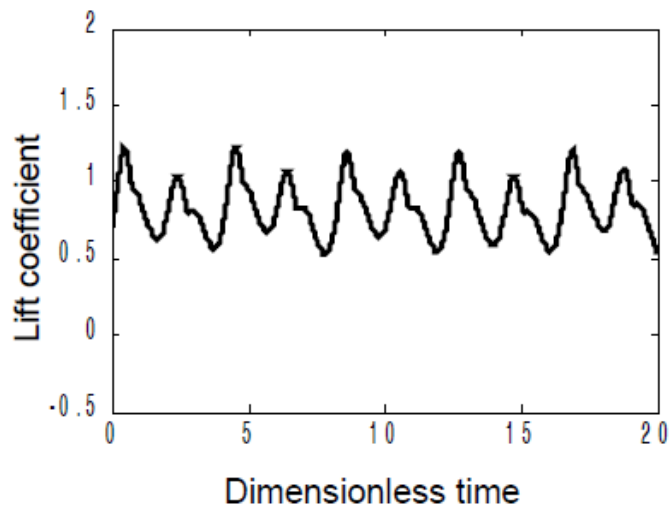


Mean drag vs. angle of attack



When using feathers, **structure (i.e, rigidity)** and **fluid time scales synchronized**.

For instance - **Lift coefficient for 22° - time and frequency domains**



Efficient structure parameters

Parameters varied during the course of the study

Angle of attack, α (degrees)	Rigidity moment, K_r	Interaction moment, K_i	Dissipation moment, K_d	Packing density, ϕ	Angular sector of movement, $[\theta_{min}, \theta_{max}]$ (degrees)	Flow frequency, ω_{fluid}
22	8.9905	0.2034	0.0909	0.0085	[-60,21]	0.4772
45	6.8002	0.2034	0.079	0.0022	[-60,60]	0.4151
70	8.9905	0.2034	0.0909	0.0085	[-60,60]	0.4772

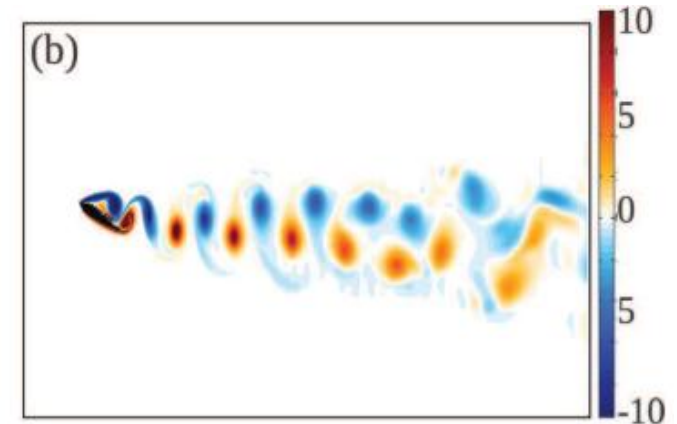
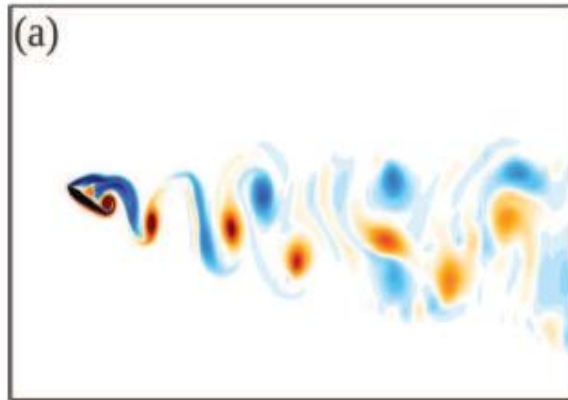
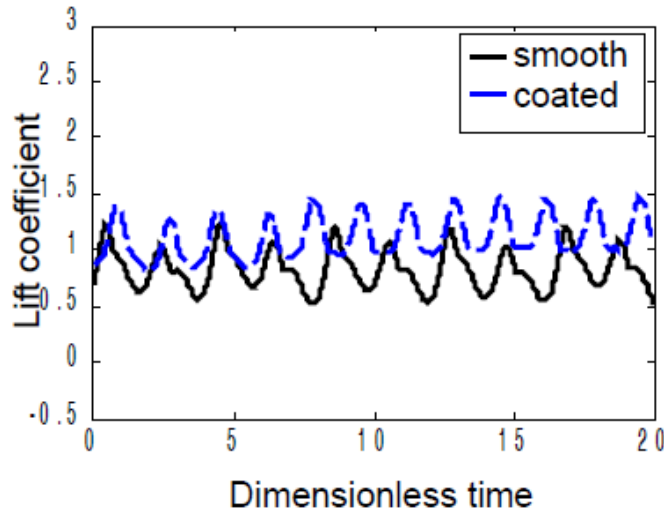
Parameters fixed throughout the course of the study

Mass of reference beam, M	12
Length of reference beam, l	8.5×10^{-2}
Diameter of reference beam, d_c	2×10^{-3}
Equilibrium angle/ Initial orientation of reference beams, θ_{eq} (degrees)	0
Extent of the coating	70% of suction side, starting 0.1 units of length after the leading edge and ending 0.2 units before the trailing edge.
Number of reference beams used, N	8

Summary of computational results [*Phys. Fluids*, 2012]

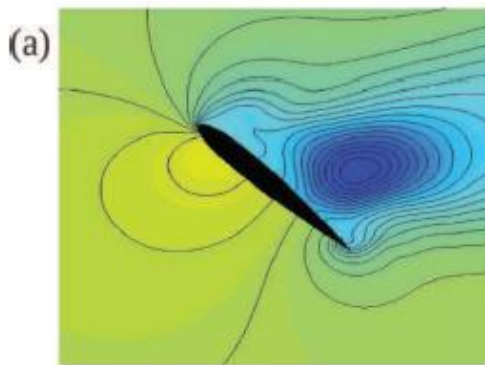
• $\alpha = 22^\circ$:

Mean lift \uparrow : **34.36%**, Lift fluctuations' \downarrow : **7.15%**, Drag fluctuations' \downarrow : **35.47%**, Mean drag \uparrow : **6.6%**

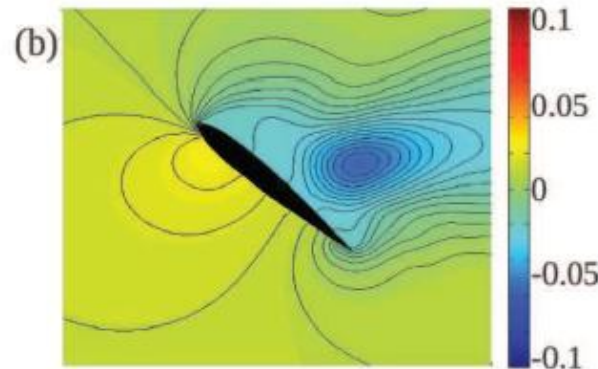


• $\alpha = 45^\circ$:

Mean drag \downarrow : **8.92%**, Drag fluctuations' \downarrow : **10.46%**, Mean lift \downarrow : **1.47%**.



$\alpha = 45^\circ$



• $\alpha = 70^\circ$:

Mean lift \uparrow : **7.5%**, Drag fluctuations' \downarrow : **9.71%**, Mean drag \downarrow : **4.92%**.

Computational modeling of fluid-structure interaction

Highlights of numerical procedure

Key computational results

Theoretical modeling for vortex-shedding

Smooth airfoil

- Development of the minimal model
- Calibration against CFD results

Airfoil with poro-elastic coating (“hairfoil”)

Motivation & development

Results, comparison with CFD & *physical* indications

Minimal models: (Airfoil) Vortex-shedding

- FINAL AIM:**
- (a) predict “optimal” structure parameters at a fraction of the cost*
 - (b) explain physical mechanism behind such optimal coatings*

Some facts

- For unsteady flows over bodies, for fixed set of parameters, long time history of lift/drag forces **periodic + independent of initial conditions**
 - i.e, lift/drag can be represented as ***self-excited oscillator***, yielding limit cycle
- ***Autonomous equations*** with ***negative linear damping*** and ***positive non-linear damping*** can produce limit cycles (as in present case)
 - i.e, small disturbances allowed to grow; large disturbances pushed back to equilibrium.

Minimal models: periodic forces in the flow past a cylinder

Hartlen & Currie (1970); Currie and Turnbull (1987)

Rayleigh oscillator $\frac{d^2 x}{dt^2} + x = \frac{dx}{dt} - \left(\frac{dx}{dt}\right)^3$

Skop & Griffin (1973)

Van der Pol-like oscillator $\frac{d^2 x}{dt^2} + x = \frac{dx}{dt} - x^2 \frac{dx}{dt}$

Nayfeh et al (2005); Akthar, Marzouk & Nayfeh (2009)

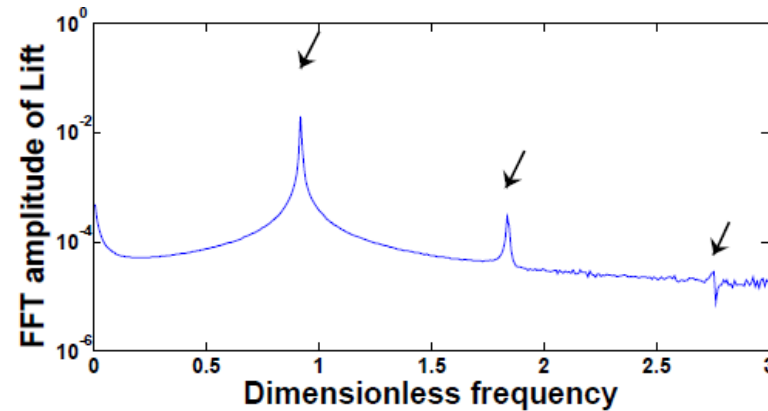
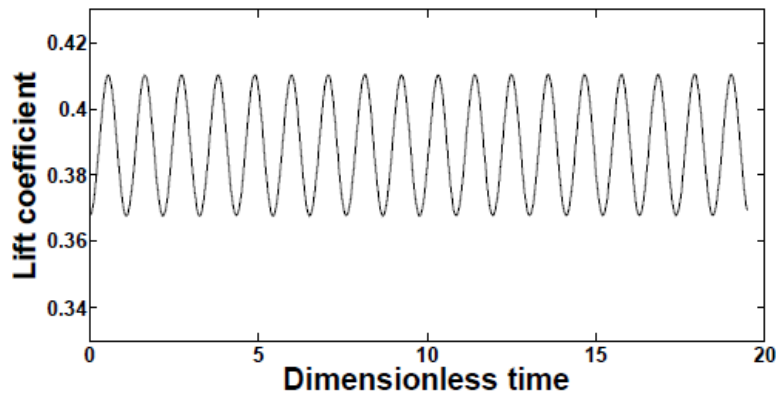
Van der Pol + Duffing-type cubic nonlinearity

$$\frac{d^2 x}{dt^2} + x = \frac{dx}{dt} - x^2 \frac{dx}{dt} - x^3$$

Crucial physics: smooth airfoil

- **Super-harmonics** of flow frequencies - peak at **twice the fundamental frequency** – unlike the case of a cylinder.

Lift coefficient for 10° - time and frequency domains

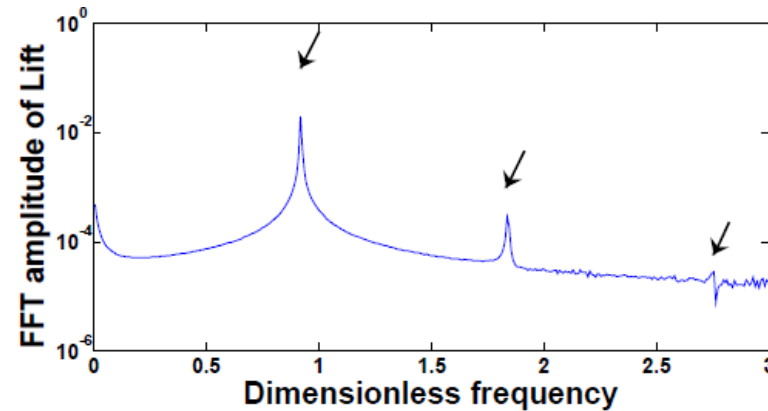
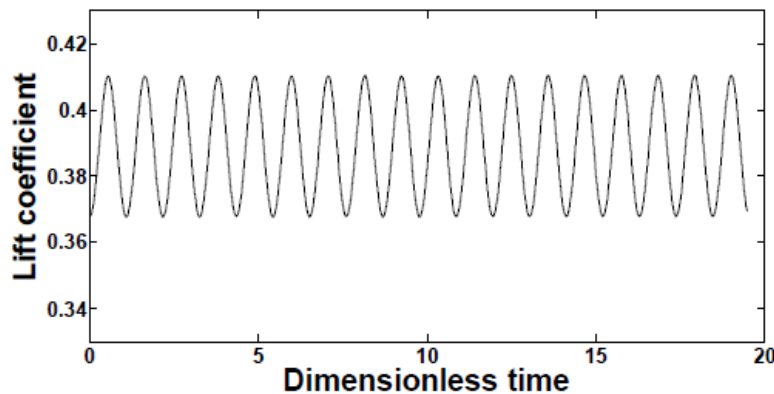


- Indicates presence of **quadratic non-linearity in model** equation.
- Can a generic equation with all possible quadratic terms be a model ?

Crucial physics: smooth airfoil

- **Super-harmonics** of flow frequencies - peak at **twice the fundamental frequency** – unlike the case of a cylinder.

Lift coefficient for 10° - time and frequency domains



- Indicates presence of **quadratic non-linearity in model** equation.
- Can a generic equation with all possible quadratic terms be a model ?
- **No, at least one higher-order non-linear term is needed to obtain a self-excited oscillator (i.e. independent of initial forcing conditions).**

When can a limit cycle exist ?

- Most general system with all possible quadratic and cubic nonlinearities, with negative linear damping:

$$\ddot{x} + x = c \dot{x} + \alpha_1 x^2 + \alpha_2 x \dot{x} + \alpha_3 \dot{x}^2 + \beta_1 x^3 + \beta_2 x^2 \dot{x} + \beta_3 x \dot{x}^2 + \beta_4 \dot{x}^3$$

When can a limit cycle exist ?

- **A necessary condition** : For most general system with all possible quadratic and cubic non-linearities with negative linear damping:

$$\ddot{x} + x = c \dot{x} + \alpha_1 x^2 + \alpha_2 x \dot{x} + \alpha_3 \dot{x}^2 + \beta_1 x^3 + \beta_2 x^2 \dot{x} + \beta_3 x \dot{x}^2 + \beta_4 \dot{x}^3$$

- **Poincaré-Lindstedt's method** guarantees the existence of a limit cycle only if

$$\alpha_2(\alpha_1 + \alpha_3) + \beta_2 + 3\beta_4 < 0$$

- Coefficients of cubic terms with odd powers of x – i.e. β_1 & β_3 – play **no role**.

(expand dependent and independent variables in powers of a small book-keeping parameter ε to have a solution uniformly valid in time, collect like-order equations, impose conditions on order zero amplitude/frequency of the solution ...)

When can a limit cycle exist ?

- **A necessary condition** : For most general system with all possible quadratic and cubic non-linearities with negative linear damping:

$$\ddot{x} + x = c \dot{x} + \alpha_1 x^2 + \alpha_2 x \dot{x} + \alpha_3 \dot{x}^2 + \beta_1 x^3 + \beta_2 x^2 \dot{x} + \beta_3 x \dot{x}^2 + \beta_4 \dot{x}^3$$

- **Poincaré-Lindstedt's method** guarantees the existence of a limit cycle only if

$$\alpha_2(\alpha_1 + \alpha_3) + \beta_2 + 3\beta_4 < 0$$

- Coefficients of cubic terms with odd powers of x – i.e. β_1 & β_3 – play **no role**.

(expand dependent and independent variables in powers of a small book-keeping parameter ε to have a solution uniformly valid in time, collect like-order equations, impose conditions on order zero amplitude/frequency of the solution ...)

When can a limit cycle exist ?

- **A necessary condition** : For most general system with all possible quadratic and cubic non-linearities with negative linear damping:

$$\ddot{x} + x = c \dot{x} + \alpha_1 x^2 + \alpha_2 x \dot{x} + \alpha_3 \dot{x}^2 + \beta_1 x^3 + \beta_2 x^2 \dot{x} + \beta_3 x \dot{x}^2 + \beta_4 \dot{x}^3$$

- **Poincaré-Lindstedt's method** guarantees the existence of a limit cycle *only if*

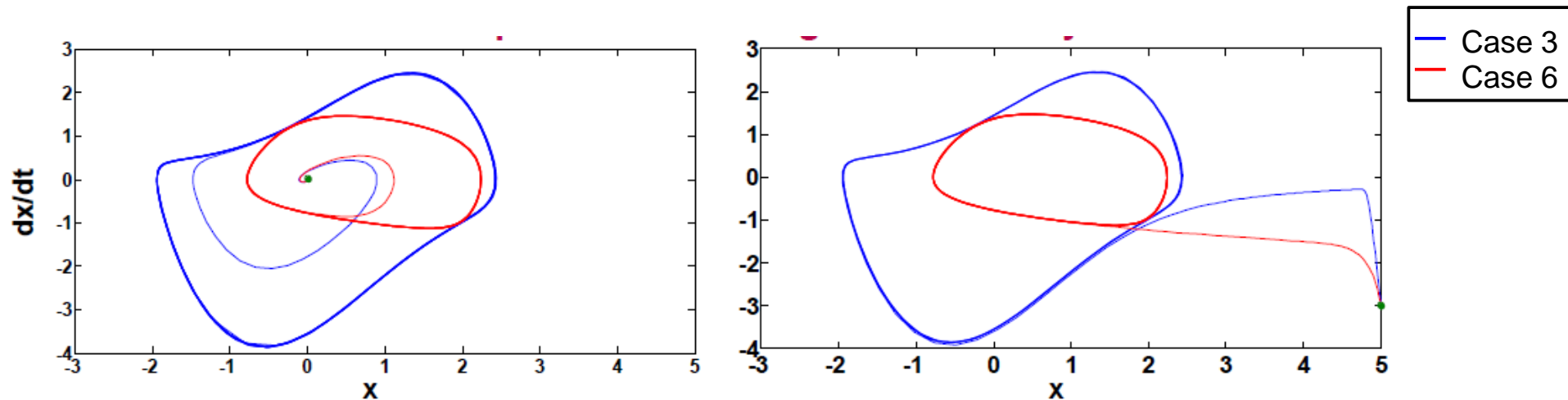
$$\alpha_2(\alpha_1 + \alpha_3) + \beta_2 + 3\beta_4 < 0$$

- Coefficients of cubic terms with odd powers of x – i.e. β_1 & β_3 – play **no role**.
- Other two cubic terms correspond to ***Rayleigh*** (as in present low-order model) & *van der Pol* oscillators resp.

Case	α_1	α_2	α_3	β_2	β_4	Existence of limit cycle
1	1	0	0	-1	0	No
2	1	0	0	0	-1	No
3	0	1	0	-1	0	Yes
4	0	1	0	0	-1	Limit cycle exists only for initial conditions with \dot{x} negative or zero.
5	0	0	1	-1	0	No
6	0	0	1	0	-1	Yes

RESULTS: *Minimal model* for smooth airfoil

Comparison of convergence to limit cycles



- Since **convergence** to the limit cycle, from both small and large initial conditions, is **faster for case 6**, the model equation is taken as:

$$\ddot{x} + x = \dot{x} + \dot{x}^2 - \dot{x}^3$$

- In the present case, since **mean lift $\neq 0$** , the equation becomes :

$$\ddot{C}_L + \omega^2 C_L = \mu \dot{C}_L - \alpha \dot{C}_L^3 + \beta \dot{C}_L^2 + \omega^2 \bar{C}_L$$

- For this equation, **method of multiple scales** used to find **right model parameters**, which in turn determine the correct model equation.

How to find a (periodic) solution?

Method of multiple scales – key steps:

- **Solutions** sought in form of **power series in δ** , where δ measures *how strongly non-linear* the system is.
- If only one time scale considered, typical issue is: for large t , perturbation solution does not match with numerical/exact solution.

Reason: Appearance of **secular terms** in perturbation solution.

- In **present problem**, *minimum three time scales* seen to be sufficient.
- Transforming model equation into 1st order complex-variable equation:

$$\dot{\zeta} = i\omega\zeta - \frac{i}{2}\omega\bar{C}_L + \frac{\delta}{2}\mu(\zeta - \bar{\zeta}) + \frac{\delta}{2}\alpha\omega^2(\zeta^3 - 3\zeta^2\bar{\zeta} + 3\zeta\bar{\zeta}^2 - \bar{\zeta}^3) + \frac{\delta}{2}\beta i\omega(\zeta^2 - 2\zeta\bar{\zeta} + \bar{\zeta}^2)$$

- Introducing three time scales $T_0 = t$, $T_1 = \delta t$ and $T_2 = \delta^2 t$, substituting

$$\zeta = \sum_{j=0}^2 \delta^j \zeta_j(T_0, T_1, T_2) + O(\delta^3)$$

and **separating** similar **coefficients** of powers of $\delta^0 (=1)$, δ^1 and δ^2 one obtains...

Finding a periodic solution (contd..)

$$D_0 \zeta_0 - i\omega \zeta_0 = \frac{-l}{2} \omega \widetilde{C}_L \quad (1)$$

$$D_0 \zeta_1 - i\omega \zeta_1 = -D_1 \zeta_0 + \frac{\mu}{2} (\zeta_0 - \bar{\zeta}_0) + \frac{\alpha}{2} \omega^2 (\zeta_0^3 - 3\zeta_0^2 \bar{\zeta}_0 + 3\zeta_0 \bar{\zeta}_0^2 - \bar{\zeta}_0^3) + \frac{\beta}{2} i\omega (\zeta_0^2 - 2\zeta_0 \bar{\zeta}_0 + \bar{\zeta}_0^2) \quad (2)$$

$$D_0 \zeta_2 - i\omega \zeta_2 = -D_2 \zeta_0 - D_1 \zeta_1 + \frac{\mu}{2} (\zeta_1 - \bar{\zeta}_1) + \frac{3\alpha}{2} \omega^2 (\zeta_0^2 \zeta_1 - \zeta_0^2 \bar{\zeta}_1 + \bar{\zeta}_0^2 \zeta_1 - \bar{\zeta}_0^2 \bar{\zeta}_1 - 2\zeta_0 \bar{\zeta}_0 \zeta_1 + 2\zeta_0 \bar{\zeta}_0 \bar{\zeta}_1) + \beta i\omega (\zeta_0 \zeta_1 - \zeta_0 \bar{\zeta}_1 - \bar{\zeta}_0 \zeta_1 + \bar{\zeta}_0 \bar{\zeta}_1) \quad (3)$$

- Substituting solution ζ_0 from (1) in (2)

+
eliminating terms proportional to $\exp(i\omega T_0)$ } \Rightarrow **bounded solution**

- Substituting ζ_0 and ζ_1 in (3), **solvability conditions** obtained } \Rightarrow **parameters of limit cycle**
- +
steady-state assumption on **amplitude of lift** coefficient

SUMMARY: Given a system, with known model parameters, characteristics of solution (i.e, amplitude, frequency, etc.) can be solved.

Conversely, given a system, with known solution, model parameters can be determined.

RESULTS: Smooth airfoil

• Final solution: $C_L(t) = a_0 + a_1 \cos(\omega_s t) + a_2 \cos(2\omega_s t) + a_3 \sin(3\omega_s t)$

where a_0 , a_1 , a_2 , a_3 and ω_s are **computational** parameters, found in terms of **model** parameters ω , μ , α and β .

• Model parameters thus recovered in terms of computational parameters as:

$$\omega = \frac{a_1^2 a_3 \omega_s}{a_1^2 a_3 - 36 a_3^3 - 6 a_2^2 a_3} \quad ; \quad \delta \mu = \frac{24 a_1 a_3^2 \omega_s}{a_1^2 a_3 - 36 a_3^3 - 6 a_2^2 a_3}$$

$$\delta \beta = \frac{6 a_2}{a_1^2} \quad ; \quad \delta \alpha = \frac{32 a_1^2 a_3 - 36 a_3^3 - 6 a_2^2 a_3}{a_1^5 \omega_s}$$

RESULTS: Smooth airfoil

- Final solution:

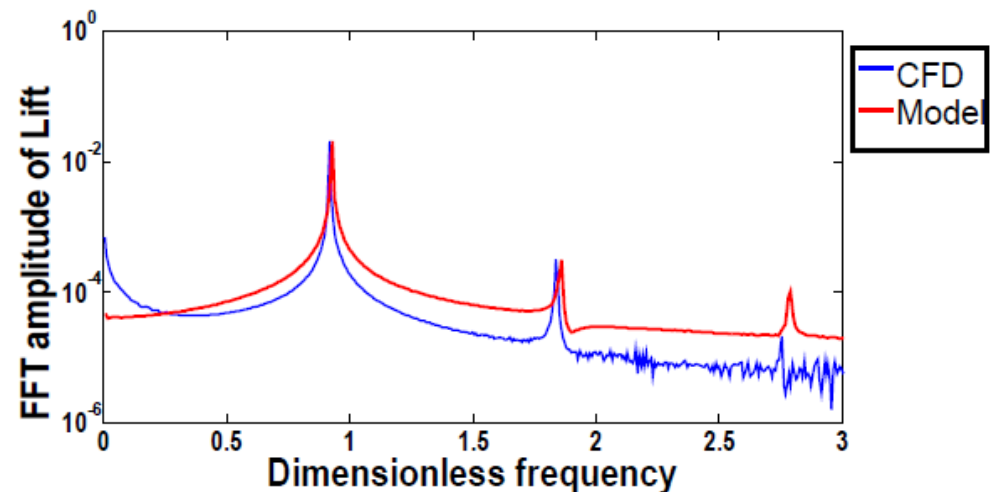
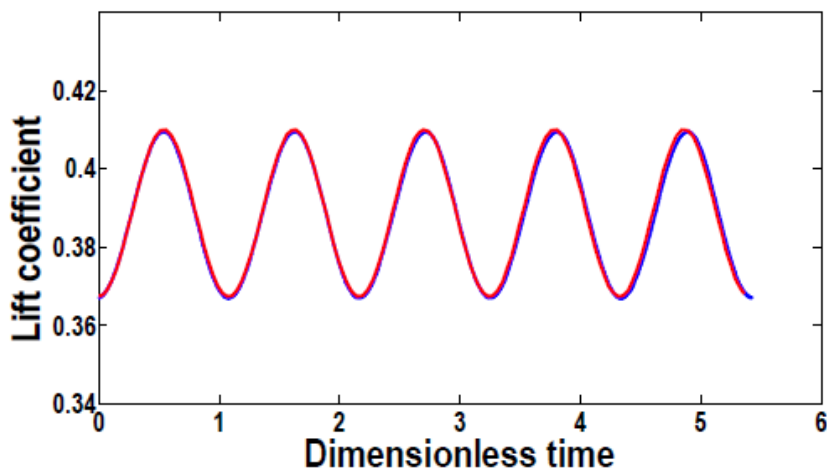
$$C_L(t) = a_0 + a_1 \cos(\omega_s t) + a_2 \cos(2\omega_s t) + a_3 \sin(3\omega_s t)$$

where a_0 , a_1 , a_2 , a_3 and ω_s are **computational** parameters, found in terms of **model** parameters ω , μ , α and β .

- Model parameters thus recovered in terms of computational parameters as:

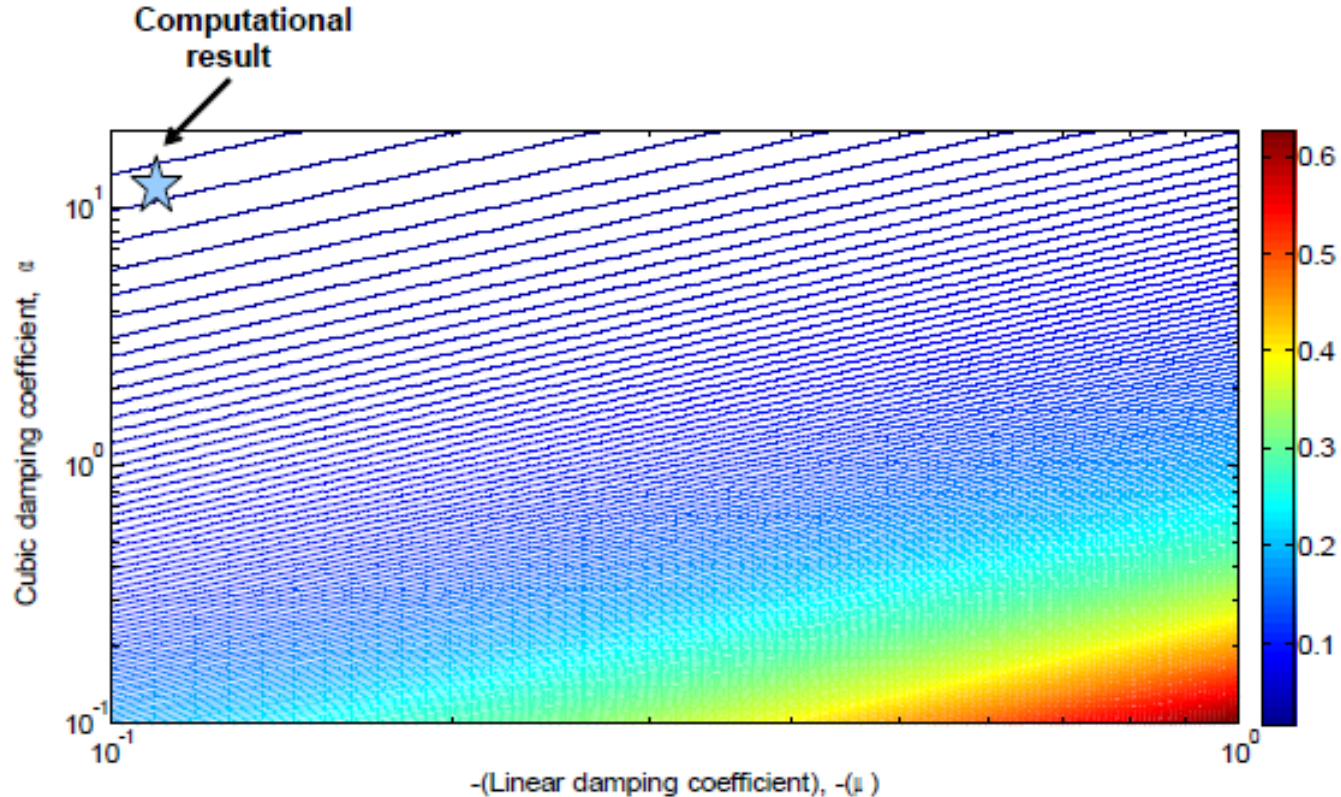
$$\omega = \frac{a_1^2 a_3 \omega_s}{a_1^2 a_3 - 36 a_3^3 - 6 a_2^2 a_3} ; \quad \delta \mu = \frac{24 a_1 a_3^2 \omega_s}{a_1^2 a_3 - 36 a_3^3 - 6 a_2^2 a_3} ; \quad \delta \beta = \frac{6 a_2}{a_1^2} ; \quad \delta \alpha = \frac{32 a_1^2 a_3 - 36 a_3^3 - 6 a_2^2 a_3}{a_1^5 \omega_s}$$

CALIBRATION



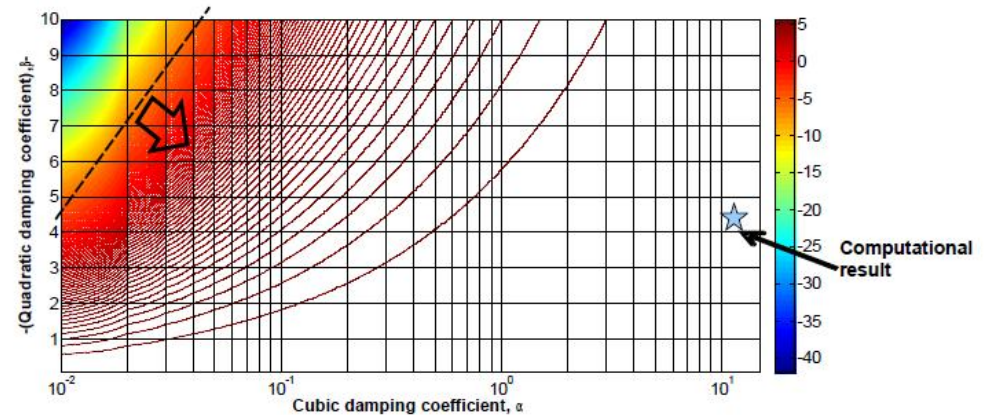
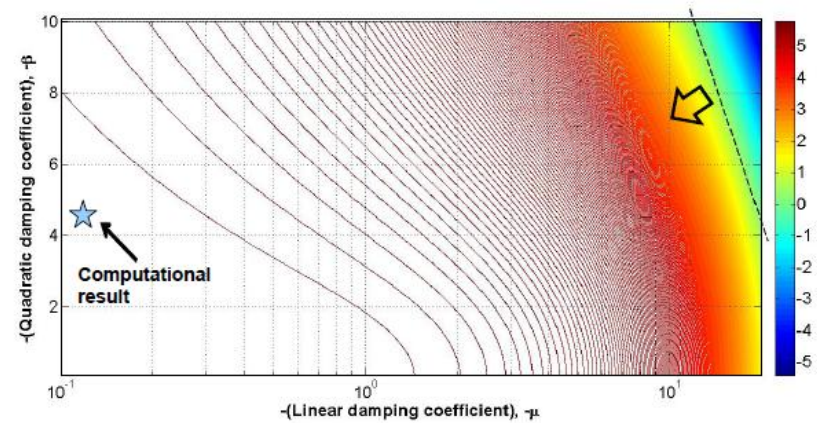
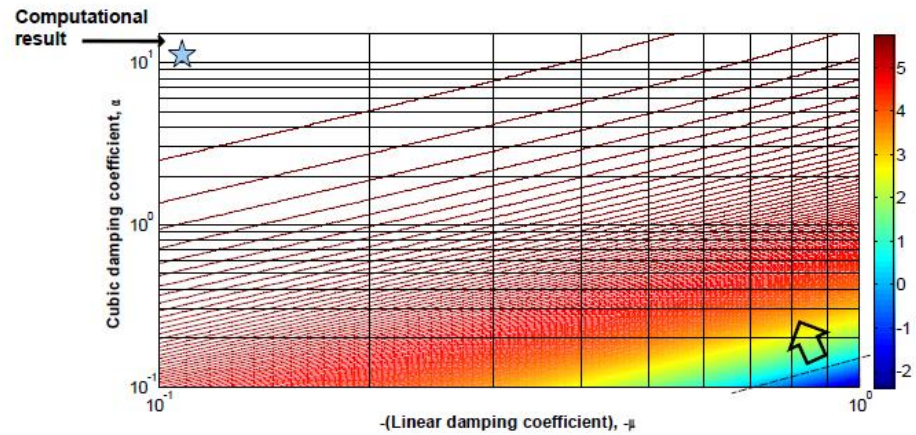
Can do *viceversa* ...

RESULTS : Dependence of amplitude a_1 on model parameters



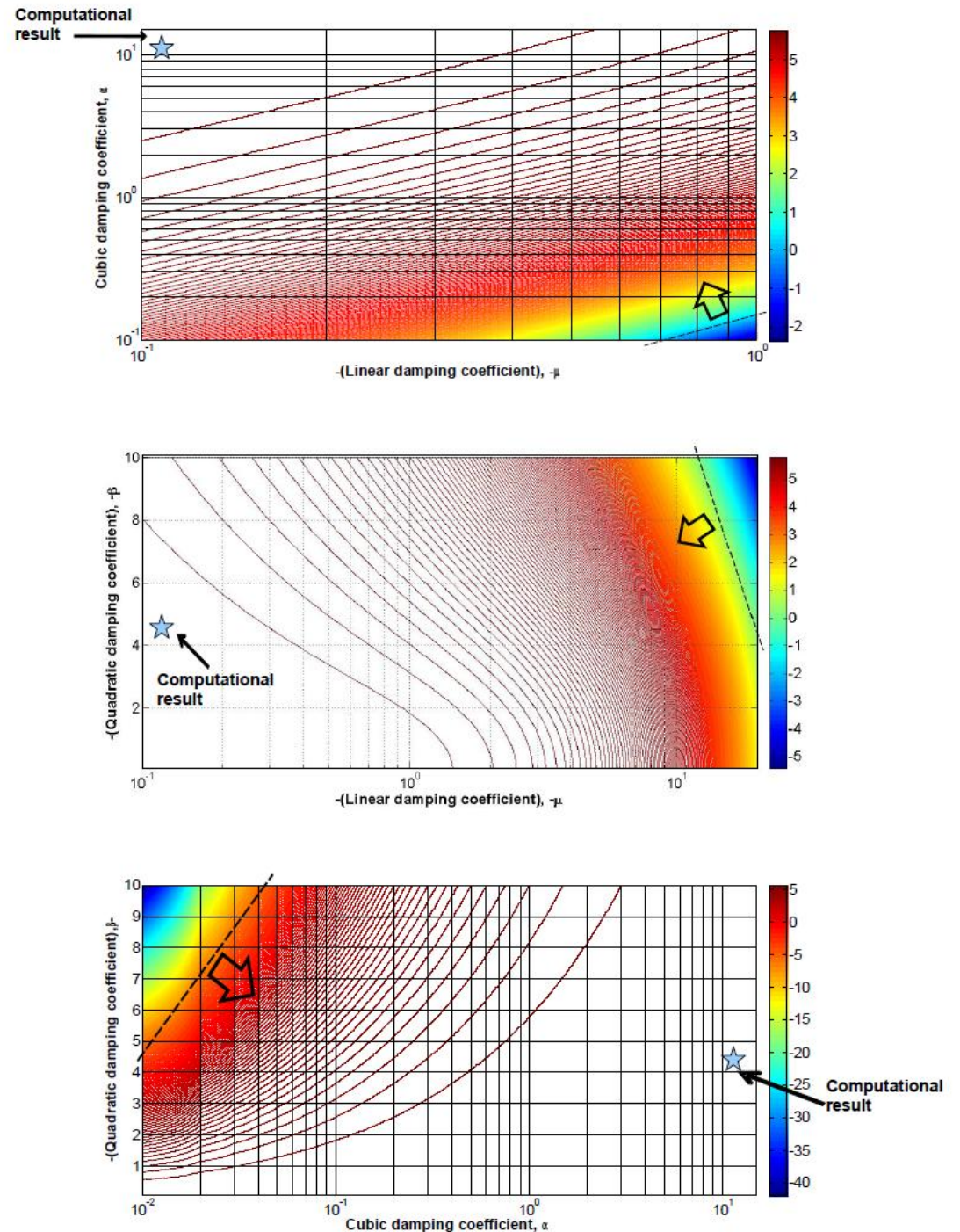
- Size of limit cycle proportional to μ / α .
- Effect of **increase in μ dominates** over increase in α .
- **Oscillations in limit cycle** scales as $\sqrt{\mu}$
- **We can easily span a very large parameter space!**

Dependence of the frequency ω_s of the limit cycle on model parameters



Dependence of the frequency ω_s of the limit cycle on model parameters

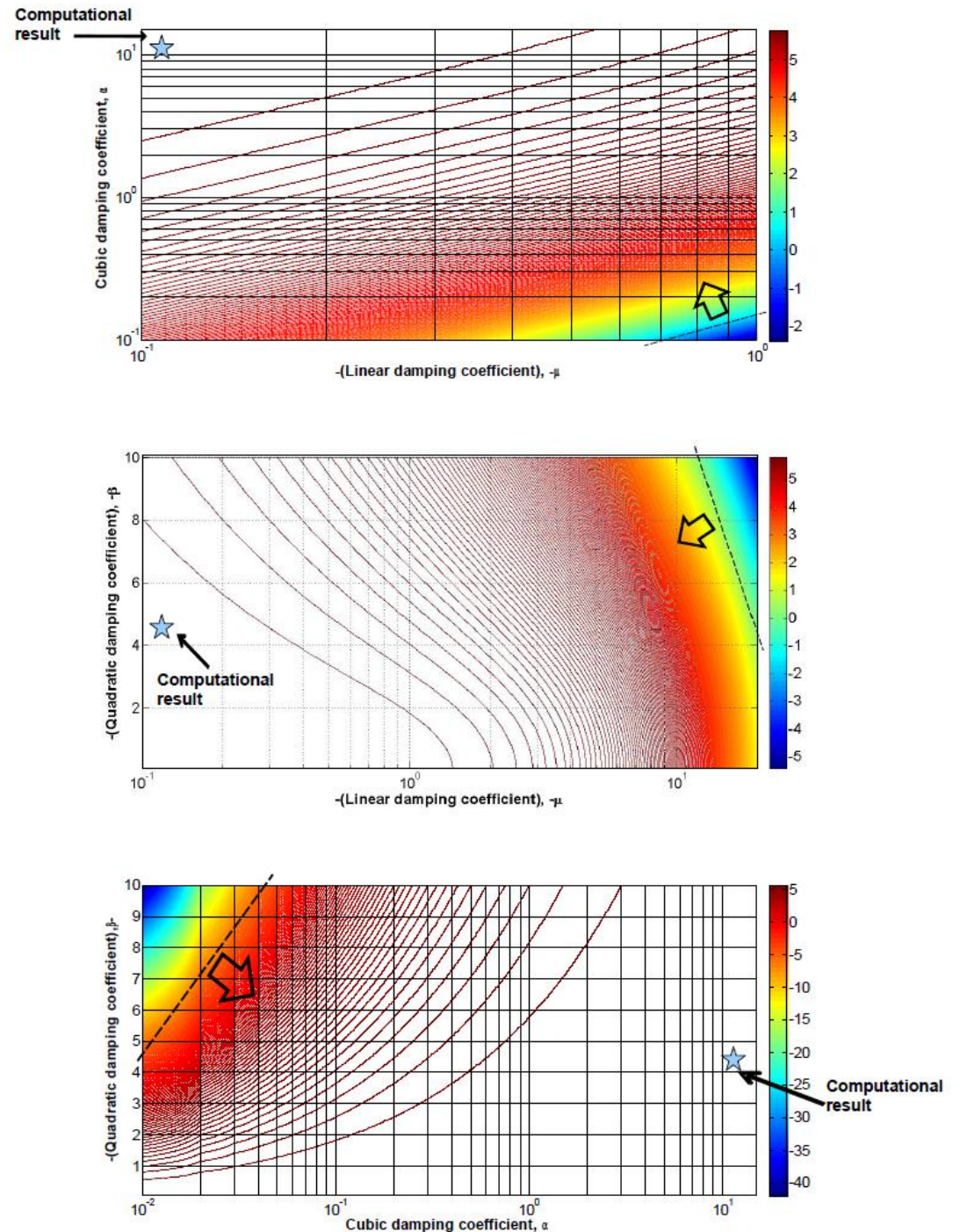
we can easily change model parameters and simulate the effect of varying Re , α , etc.



Dependence of the frequency ω_s of the limit cycle on model parameters

we can easily change model parameters and simulate the effect of varying Re , α , etc.

... and even uncover unphysical solutions ...



Computational modeling of fluid-structure interaction

Highlights of numerical procedure

Key computational results

Theoretical modeling for vortex-shedding

Smooth airfoil

Development of the minimal model

Calibration against CFD results

- ***Airfoil with poro-elastic coating (“hairfoil”)***
 - Motivation & development
 - Results, comparison with CFD & *physical* indications

COATED AIRFOIL: *towards a low-order model*

Some questions:

- What are (the) **optimal** structure **parameters** ?
- How are structure **parameters** related to **aerodynamic changes** ?
- e.g, why do *some* feathers lead to drag reduction *and/or* lift enhancement, etc.?
- Which structure parameters are **most crucial** for **realistic physics** ?
- e.g, in computations,
 - features modeled with compliance, porosity and anisotropy
 - rigidity effects were predominant.
- Simplest model for coupled fluid-structure system:

$$\begin{aligned} \ddot{C}_L + \omega^2 C_L - \omega^2 \widetilde{C}_L - \mu \dot{C}_L + \alpha \dot{C}_L^3 - \beta \dot{C}_L^2 &= \rho_1 \theta \\ \ddot{\theta} + c \dot{\theta} + \omega_1^2 \theta &= \rho_2 (C_L - \widetilde{C}_L) \end{aligned}$$

- The **method of multiple scales** again yields insights!

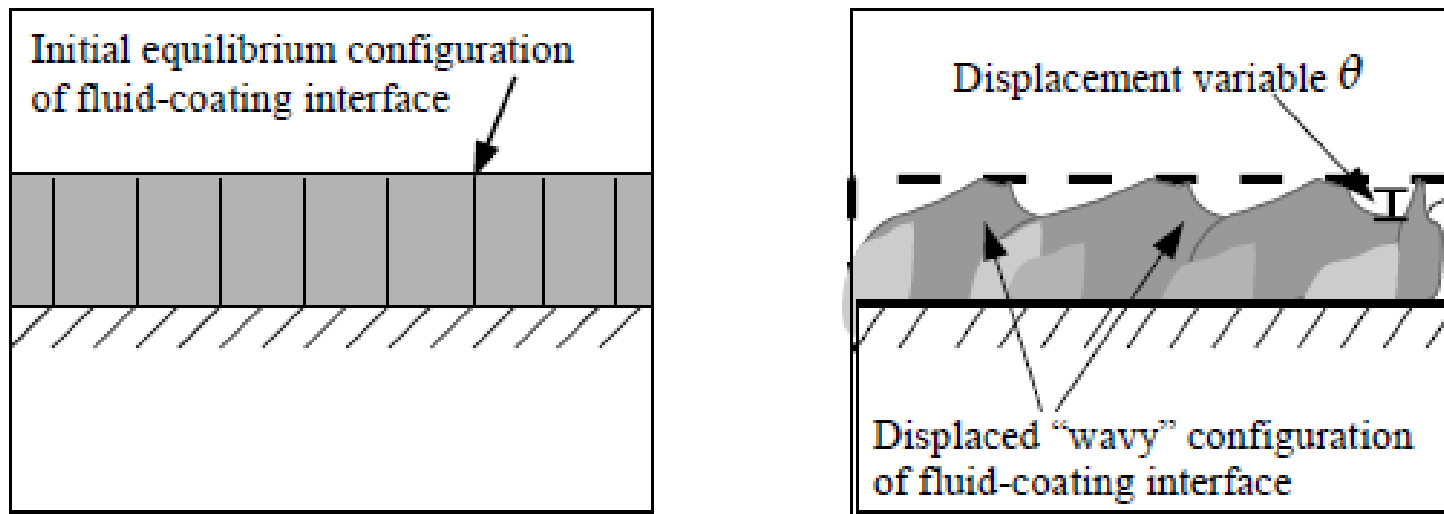


Figure 1: Fluid-coating interface : (left) - initial undisturbed configuration (i.e., without any forcing from the fluid) - the vertical lines here denote a discrete number of feathers spread uniformly in this layer; (right) - disturbed configuration showing the displacement variable θ . Note here that the colour gradient in this disturbed layer characterizes the non-uniform, time-varying porosity (i.e., darker shades denote clustering of feathers while lighter shades stand for areas with a lower instantaneous concentration of feathers).

$$\ddot{C}_L + \omega^2 C_L - \omega^2 \bar{C}_L - \mu \dot{C}_L + \alpha \dot{C}_L^3 - \beta \dot{C}_L^2 = \rho_1 \theta$$

$$\ddot{\theta} + c \dot{\theta} + \omega_1^2 \theta = \rho_2 (C_L - \bar{C}_L)$$

Solution of coupled system

- Similar procedure as for smooth airfoil – but now for both equations.
- Three time scales (as before).
- Separating similar coefficients of powers of δ^0 (=1), δ^1 and δ^2 and solving.
- **Constraints analogous to case of smooth airfoil :**
 - Vanishing of secular terms in closed-form solution of lift.
 - Steady-state assumption on amplitude of lift coefficient $a_1(\mathbf{t})$.

$$\frac{\mu}{2} a_1(t) - \frac{3}{8} \alpha \omega^2 a_1^3(t) = 0$$

- **Additional, but similar, constraints** now also on poroelastic coating deformation $a_2(\mathbf{t})$.

$$c a_2(t) = 0$$

RESULTS : Weak structure → fluid coupling

- **Case 1:** $a_1(t) = \frac{2}{\omega} \sqrt{\frac{\mu}{3\alpha}}$; $a_2(t) = 0$ (i.e, c can be arbitrarily large)

$$C_L(t) = \widetilde{C}_L + \frac{2\delta\beta\mu}{3\alpha\omega^2} + \sqrt{\frac{4\mu}{3\alpha\omega^2}} \cos(\omega_{s,1}t) + \frac{2\delta\beta\mu}{9\alpha\omega^2} \cos(2\omega_{s,1}t) + \delta \sqrt{\frac{\mu^3}{432\alpha\omega^4}} \sin(3\omega_{s,1}t)$$

$$\theta(t) = \frac{-2\delta\rho_2}{\omega(\omega - \omega_1)(\omega + \omega_1)} \sqrt{\frac{\mu}{3\alpha}} \cos(\omega_{s,1}t)$$

where

$$\omega_{s,1} = \omega - \frac{(\delta\mu)^2}{16\omega} - \frac{2(\delta\beta)^2\mu}{9\alpha\omega} - \frac{(\delta\rho_1)(\delta\rho_2)}{2\omega(\omega - \omega_1)(\omega + \omega_1)}$$

NOTE:

- Form of $C_L(t)$ exactly **similar to** case of **smooth airfoil (with super-harmonics)**.
- **No super-harmonics** of $\omega_{s,1}$ in dynamics of $\theta(t)$.
- **Resonant condition** : If $\omega_{s,1} \approx 0$ (i.e, $\omega \sim \omega_1$), $\sqrt{\frac{4\mu}{3\alpha\omega^2}}$ dominates, **mean lift** ↑
- **Non-resonant condition** : Changes in structure parameters **do not directly change** lift →

THE STRUCTURE IS SLAVED BY THE FLUID

RESULTS : Weak fluid → structure coupling

• **Case 2:** $a_1(t) = 0$; $c = 0$ (i.e, $a_2(t)$ can be arbitrary → C_0)

$$C_L(t) = \widetilde{C}_L + \frac{\delta\rho_1 C_0}{(\omega - \omega_1)(\omega + \omega_1)} \cos(\omega_{s,2}t)$$

$$\theta(t) = C_0 \cos(\omega_{s,2}t)$$

where $\omega_{s,2} = \omega_1 - \frac{(\delta\rho_1)(\delta\rho_2)}{2\omega_1(\omega - \omega_1)(\omega + \omega_1)}$ (i.e, $\omega_{s,2}$ a perturbation of ω_1).

NOTE :

- Dynamics of coupled system dictated by structure frequency.
- **No superharmonics** of $\omega_{s,2}$ in $C_L(t)$ and $\theta(t)$.
- **Resonant condition** : If $\omega_{s,2} \approx 0$ (i.e, $\omega \sim \omega_1$), mean lift ↑ by $O(\delta)$ when:
 - structure-fluid coupling parameter ρ_1 increased (**decrease porosity**).
 - **increase compliance** so that steady state oscillations of feather C_0 is large.
- **Non-resonant condition** : Lift fluctuations ↓ if $\frac{\delta\rho_1 C_0}{(\omega - \omega_1)(\omega + \omega_1)} < \sqrt{\frac{4\mu}{3\alpha\omega^2}}$

NEVER REALISED IN PRACTISE WITH IBM SIMULATIONS

RESULTS : Two-way coupling

Case 3: $a_1(t) = \frac{2}{\omega} \sqrt{\frac{\mu}{3\alpha}}$; $c = 0$ (i.e, $a_2(t)$ can be arbitrarily large)

$$C_L(t) = \widetilde{C}_L + \frac{2\delta\beta\mu}{3\alpha\omega^2} + \sqrt{\frac{4\mu}{3\alpha\omega^2}} \cos(\omega_{s,1}t) + \frac{2\delta\beta\mu}{9\alpha\omega^2} \cos(2\omega_{s,1}t) + \delta \sqrt{\frac{\mu^3}{432\alpha\omega^4}} \sin(3\omega_{s,1}t) + \frac{\delta\rho_1 C_0}{(\omega - \omega_1)(\omega + \omega_1)} \cos(\omega_{s,2}t)$$

$$\theta(t) = C_0 \cos(\omega_{s,2}t) - \frac{2\delta\rho_2}{\omega(\omega - \omega_1)(\omega + \omega_1)} \sqrt{\frac{\mu}{3\alpha}} \cos(\omega_{s,1}t)$$

NOTE:

- **Solution** – combination of solutions of **cases 1 and 2**.
- **No super-harmonics** of $\omega_{s,1}$ in dynamics of $\theta(t)$.
- **No superharmonics** of $\omega_{s,2}$ in $C_L(t)$ and $\theta(t)$.
- **Resonant condition** : If $\omega_{s,1}$ and $\omega_{s,2} \approx 0$, mean lift \uparrow by $O(\delta)$ as in **Case 2**.
- **Non-resonant condition** : **Increase in lift fluctuations avoided** as in **Case 2**.

Model parameters from CFD results

Re-writing the most general form of analytical solution (i.e, Case 3) as:

$$C_L(t) = l_0 + l_1 \cos(\omega_{s,1}t) + l_2 \cos(2\omega_{s,1}t) + l_3 \sin(3\omega_{s,1}t) + l'_1 \cos(\omega_{s,2}t)$$

$$\theta(t) = \theta_1 \cos(\omega_{s,2}t) + \theta'_1 \cos(\omega_{s,1}t)$$

one gets the following coupled quadratic equations for the frequencies ω and ω_1

$$(l_1^2 l_3 - 36 l_3^3 - 6 l_2^2 l_3) \omega^2 - l_1^2 l_3 \omega_{s,1} \omega - l_1^2 l_3 \omega_1^2 + l_1^2 l_3 \omega_{s,2} \omega_1 = 0$$

$$(2 \theta_1 l_1 - l'_1 \theta'_1) \omega_1^2 - 2 \omega_{s,2} \theta_1 l_1 \omega_1 + l'_1 \theta'_1 \omega^2 = 0$$

and the following six equations:

$$\delta \mu = \frac{24 l_3 \omega}{l_1} \quad ; \quad \delta \beta = \frac{6 l_2}{l_1^2} \quad ; \quad \delta \alpha = \frac{32 l_3}{l_1^3 \omega} \quad ; \quad C_0 = \theta_1 \quad ;$$

$$\delta \rho_1 = \frac{(\omega - \omega_1)(\omega + \omega_1) l'_1}{C_0} \quad ;$$

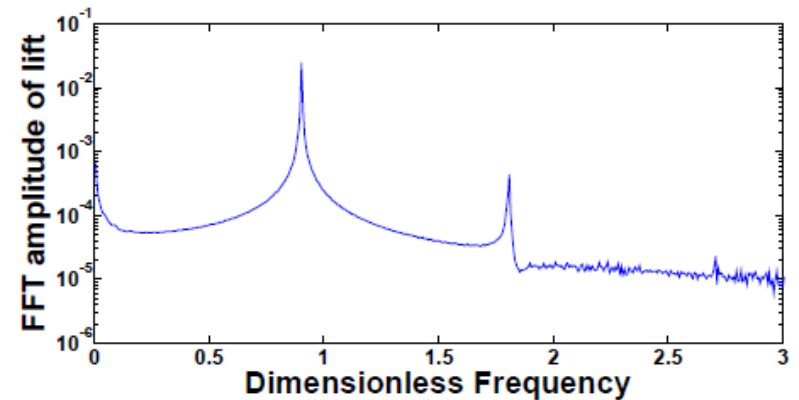
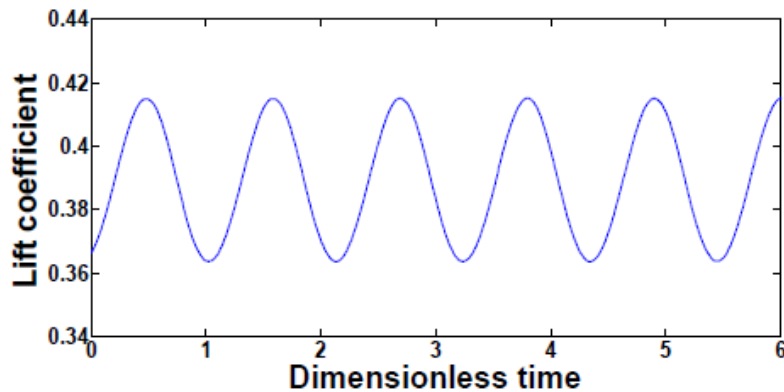
$$\delta \rho_2 = \frac{-\omega(\omega - \omega_1)(\omega + \omega_1) \theta'_1}{2} \sqrt{\frac{3 \alpha}{\mu}}$$

Comparison: *minimal model* and CFD

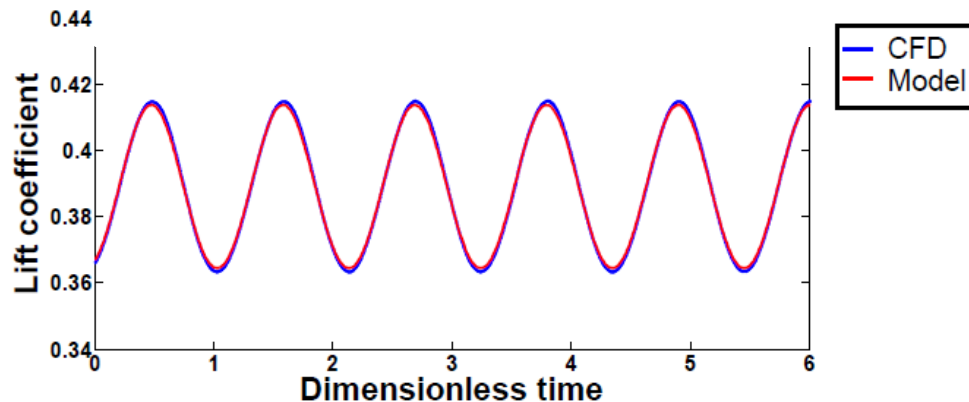
- **CASE:** Airfoil with a poro-elastic coating in **front half** of its **suction side**:



- Lift coefficient – time and frequency domains:



- Correspondence with **Case 1**, i.e. case with only $\omega_{s,1}$ and super-harmonics.



Computational modeling of fluid-structure interaction

Highlights of numerical procedure

Key computational results

Theoretical modeling for vortex-shedding

Smooth airfoil

Theory & development

Results and comparison with CFD results

- ***Airfoil with poro-elastic coating (“hairfoil”)***

Motivation & development

Results, comparison with CFD & *physical* indications

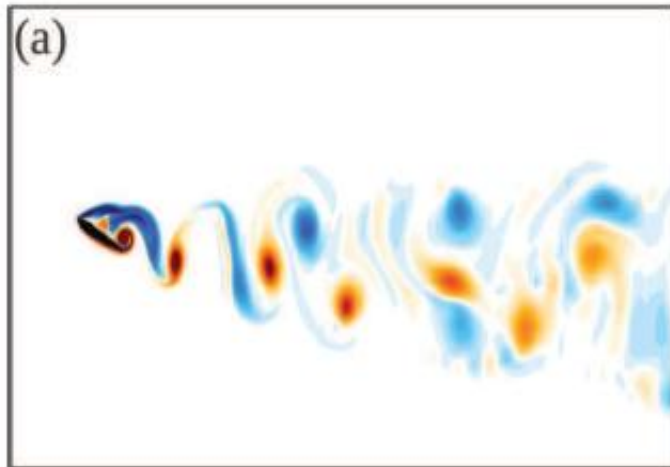
- ***Summary & future extensions***

SUMMARY

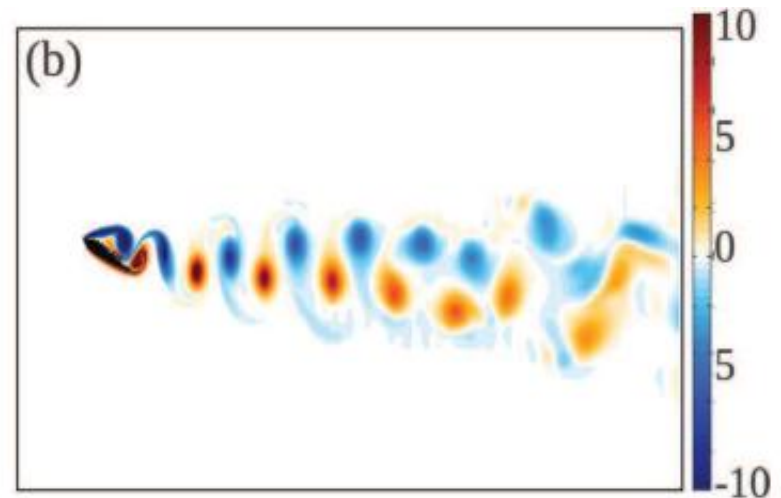
• Computational modeling of fluid-structure interaction

- Computational investigation of low Reynolds number flows.
- Employment of immersed boundary method for complex, moving boundaries.
- Synchronization of structure frequency with fluid frequency can:
 - affect flow topology near airfoil, by spontaneous adjustment;
 - modify vortex-shedding;
 - change pressure distribution for the better.

Without coating



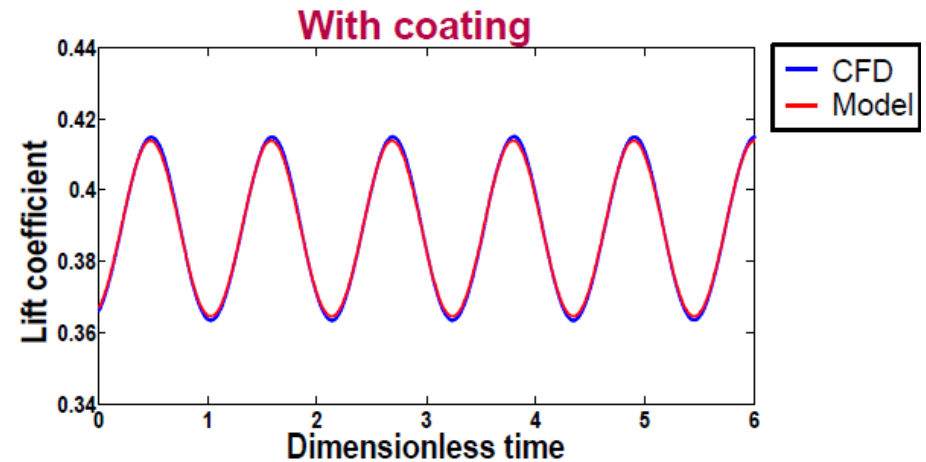
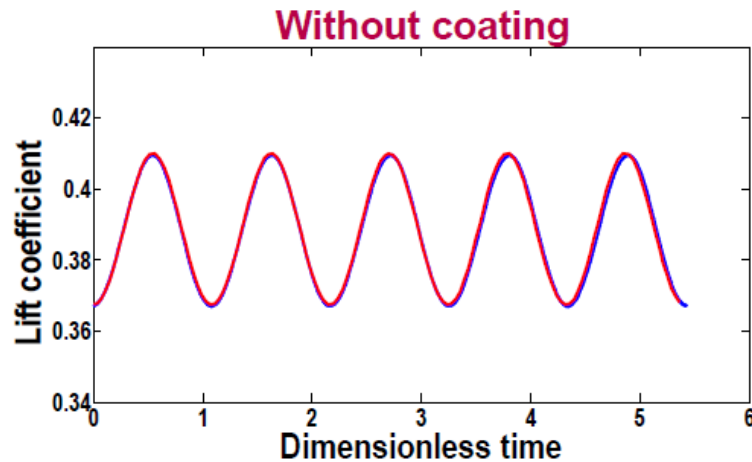
With coating



SUMMARY

Theoretical modeling for vortex-shedding

- Non-linear minimal models developed for vortex-shedding behind :
 - smooth airfoil;
 - airfoil with poro-elastic coating.
- These models are capable of :
 - reproducing dynamics obtained by heavy computations;
 - giving insights into prediction of optimal structure parameters.



FUTURE EXTENSIONS & PERSPECTIVES

- ***Non-linear model*** for structure part.
- ***Bending feathers***: Bending also neglected since feathers were short enough - usually the case with birds' coverts.
- Effectiveness of coating under ***turbulent conditions***, particularly vis-a-vis control of transition to turbulence.
- For higher Reynolds number regimes meaningful to add a third spatial component ...
- Modeling of hairy actuators on ***internal flow without vortex-shedding***
Eg:- Couette flow.
- How do actuators affect velocity profile in boundary layer ?
- Effectiveness of coating on ***more complex configurations*** –
 - asymmetric airfoils (with positive camber)
 - dynamic airfoils (with slow pitching and/or heaving, dynamically changing camber).

Ajit Niranjan



The Times of India, April 16 2009

Immersed boundary force

- Feedback forcing term in N-S \leftrightarrow **Spring-mass system** equilibrium.

$$F = \alpha \int (U^{des} - U) dt + \beta (U^{des} - U)$$

- Spring constant α **not large** – else, spring breaks.
- Damping parameter β **not large** – else, force less reactive.
- Magnitudes of these constants in buffer zone must ensure **no dominant frequency enters inflow**, when domain is streamwise periodic.

